

Dynamic and Stability Assessment of an Automatic Voltage Regulator Based on Time- and Frequency-Domain Analysis

I Ketut Wiryajati¹, Supriyatna¹, Firda Amelia¹

¹ Department of Electrical Engineering, Faculty of Engineering, University of Mataram
Jl. Majapahit No. 62, Mataram 83125, West Nusa Tenggara, Indonesia

ARTICLE INFO

Article history

Received Desember 2, 2026
Revised Januari 28, 2026
Accepted February 28, 2026

Keywords

Automatic Voltage Regulator;
PID controller;
time-domain analysis;
frequency-domain analysis;
power system stability.

ABSTRACT

This study presents a dynamic and stability analysis of an Automatic Voltage Regulator (AVR) system for a synchronous generator using time-domain and frequency-domain approaches. The system is modelled as a series of first-order linear subsystems consisting of an amplifier, exciter, generator, and feedback sensor, resulting in a fourth-order closed-loop system. Numerical simulations are conducted to compare the performance of the AVR without a controller and with a PID controller. Time-domain analysis indicates that the uncontrolled system exhibits a rise time of 0.339 s, an overshoot of 57.937%, and a damping ratio of approximately 0.17, indicating a heavily underdamped response. After implementing the PID controller, the rise time decreases to 0.295 s and the overshoot is significantly reduced to 14.368%, with the damping ratio increasing to approximately 0.53.

Frequency-domain analysis using Bode diagrams shows an improvement in phase margin from less than 20° to more than 40°, and gain margin from below 6 dB to above 10 dB. The dominant pole shifts from approximately $\text{Re}(s) \approx -0.2$ to $\text{Re}(s) \approx -1.0$ in the complex plane, confirming enhanced relative stability and faster transient decay. Overall, the results demonstrate that the PID controller significantly improves stability, response speed, and damping performance, making it suitable for voltage regulation in power system applications

corresponding Author:

I Ketut Wiryajati, Department of Electrical Engineering, Faculty of Engineering, University of Mataram
Jl. Majapahit No. 62, Mataram 83125, West Nusa Tenggara, Indonesia.
Email: kjatiwirya@unram.ac.id

1. INTRODUCTION

Modern power systems require stable and reliable voltage quality to ensure continuity of power supply for industrial, commercial, and critical loads[1]. One of the main components responsible for maintaining the voltage stability of a synchronous generator is the Automatic Voltage Regulator (AVR) [2]. The AVR functions to control the generator output voltage by regulating the excitation current so that voltage fluctuations caused by load variations and system disturbances can be minimized[3][4]. Instability in the AVR system may lead to voltage oscillations[5], excessive overshoot[6][7], and prolonged settling time, which ultimately degrade power quality and increase the risk of wider system disturbances[8].

Various studies indicate that the dynamic characteristics of an AVR are strongly influenced by the controller parameters employed. Conventional AVR systems generally utilize a Proportional-Integral-Derivative (PID) controller due to its simple structure and ease of implementation[9][10]. However, improper tuning of PID parameters may result in low stability margins and inadequate transient response. A study published in the International Journal of Power Electronics and Drive Systems (IJPEDS) by IAES (Institute of Advanced Engineering and Science) reported that conventional tuning methods such as Ziegler–Nichols often produce high overshoot and relatively small phase margins in nonlinear AVR systems[11]. Similar findings were reported in the Bulletin of Electrical Engineering and Informatics (BEEI), stating that AVR systems without further optimization exhibit limited gain margins and are vulnerable to parameter disturbances [12].

With the development of intelligent optimization approaches, various methods such as Particle Swarm Optimization (PSO) [13], Genetic Algorithm (GA) [14], and Fuzzy Logic[15] have been applied to improve

AVR performance. Research published in the International Journal of Electrical and Computer Engineering (IJECE) (IAES, 2021) demonstrated that integrating PID with optimization algorithms can increase the phase margin by more than 25° compared to non-optimized systems[16]. Furthermore, an international study published in IEEE Access (2020) reported that hybrid PID–metaheuristic approaches significantly reduce settling time and enhance robustness against load variations[17]. These findings indicate that improvements in stability margins (gain margin and phase margin) constitute important indicators in evaluating the control quality of AVR systems.

Despite the development of various optimization approaches, a research gap remains in the comprehensive frequency-domain-based stability margin analysis. Many studies emphasize time-domain parameters (rise time, settling time, overshoot), yet do not thoroughly analyze dominant pole shifts and improvements in gain margin and phase margin through Bode diagrams and root locus methods. In modern control theory, stability margins represent a primary indicator of system robustness against model uncertainties. Therefore, research is required to systematically compare AVR performance before and after PID controller implementation using an integrated time-domain and frequency-domain analysis.

This study proposes a structured analytical approach by conducting a comprehensive evaluation of AVR system responses both without a controller and with a PID controller. The analysis is carried out by comparing transient parameters (rise time, overshoot, settling time, steady-state error) and evaluating stability margins using Bode diagrams to determine gain margin and phase margin. Additionally, dominant pole identification is performed to understand the damping characteristics of the system after PID implementation. Through this approach, the study not only quantifies performance improvement numerically but also explains the dynamic mechanisms underlying such enhancement.

The main contribution of this research lies in integrating time-domain and frequency-domain analyses in evaluating AVR performance, thereby providing a comprehensive perspective on system robustness improvement. Moreover, this study presents quantified stability margin enhancement as an objective indicator of control performance improvement. The results are expected to provide a technical reference for the development of more stable and adaptive generator excitation systems, particularly in medium- to large-scale power systems.

The objectives of this study are: (1) to model the AVR system in the form of a representative transfer function; (2) to analyze the system response without a controller as a baseline condition; (3) to design and implement a PID controller to improve system performance; (4) to compare performance parameters in both time and frequency domains; and (5) to measure the improvement in gain margin and phase margin as indicators of enhanced system stability.

Accordingly, this research offers a problem-solving solution in the form of improved stability and robustness of the AVR system through PID control optimization based on comprehensive analysis. This approach is expected to provide both scientific and practical contributions to the development of generator voltage regulation systems that are more reliable and responsive to the dynamics of modern power systems.

2. METHOD

This study employs an analytical–quantitative approach based on mathematical modeling and numerical simulation to analyze the dynamic characteristics and stability of an Automatic Voltage Regulator (AVR) system in a synchronous generator. The main focus of this research is to evaluate the system response in the time domain and its stability characteristics in the frequency domain, thereby obtaining a comprehensive understanding of the voltage regulation system performance.

The initial stage of the study involves mathematical modeling of each AVR subsystem, consisting of the amplifier (Equation (2)), exciter (Equation (3)), generator (Equation (4)), and feedback sensor (Equation (5)). Each subsystem is modeled as a first-order linear system represented in transfer function form. In general, the transfer function of each block can be expressed as Equation (1):

$$G_i(s) = \frac{K_i}{\tau_i s + 1} \quad (1)$$

where $G_i(s)$ is the transfer function of the i -th subsystem in the Laplace domain, K_i is the steady-state gain of the subsystem, τ_i is the subsystem time constant (indicating the dynamic response speed), and s is the Laplace complex variable. This equation represents a first-order system with a single pole at $s = -1/\tau_i$. The smaller the value of τ_i , the faster the system response.

$$G_A(s) = \frac{K_A}{\tau_A s + 1} \quad (2)$$

$$G_E(s) = \frac{K_E}{\tau_E s + 1} \quad (3)$$

$$G_G(s) = \frac{K_G}{\tau_G s + 1} \quad (4)$$

$$G_S(s) = \frac{K_S}{\tau_S s + 1} \quad (5)$$

Where K_A is the voltage amplifier gain and τ_A is the amplifier time constant. The amplifier strengthens the error signal before it is forwarded to the exciter. K_E is the excitation system gain and τ_E is the excitation time constant. The exciter regulates the rotor field current that influences the generator output voltage.

K_G is the generator dynamic gain and τ_G is the generator time constant. Equation (4) represents the terminal voltage dynamics of the generator in response to field current variations.

K_S is the sensor gain and τ_S is the sensor time constant. The sensor acts as a voltage measurement element and generates the feedback signal. The transfer function of the AVR plant without feedback is obtained by multiplying the three main blocks amplifier, exciter, and generator resulting in:

$$G(s) = G_A(s)G_E(s)G_G(s) \quad (6)$$

where $G(s)$ is the overall plant transfer function without feedback, representing the relationship between the error signal and the generator terminal voltage. Since each block is a first-order system, the overall plant becomes a third-order system.

By considering the sensor as a negative feedback path, the closed-loop transfer function can be formulated as:

$$T(s) = \frac{G(s)}{1 + G(s)G_S(s)} \quad (7)$$

where $T(s)$ is the closed-loop transfer function and $1 + G(s)G_S(s)$ is the characteristic equation of the system. The roots of the characteristic equation determine the closed-loop pole locations.

Equation (7) forms the basis for the overall dynamic and stability analysis of the system. Time-domain analysis is performed by applying a unit step input to the closed-loop system. The output response is evaluated using standard control performance parameters, namely rise time (t_r), settling time (t_s), percentage overshoot (M_p) in Equation (8), and steady-state error (SSE). The overshoot value is calculated using Equation (8):

$$M_p = \frac{y_{max} - y_{ss}}{y_{ss}} \times 100\% \quad (8)$$

where y_{max} is the peak response value and y_{ss} is the steady-state value. Furthermore, the damping ratio (ζ) can be estimated using Equation (9):

$$\zeta = \frac{-\ln(M_p/100)}{\sqrt{\pi^2 + \ln^2(M_p/100)}} \quad (9)$$

where ζ is the system damping ratio. It is used to identify oscillatory characteristics: $\zeta < 1 \rightarrow$ underdamped system, $\zeta = 1 \rightarrow$ critically damped, $\zeta > 1 \rightarrow$ overdamped

The value of ζ is directly related to the relative stability of the system and is used to interpret oscillatory behavior based on the equivalent second-order system theory.

Subsequently, stability analysis is performed in the frequency domain using the Bode diagram approach and stability margin analysis. The open-loop transfer function is defined as:

$$L(s) = G(s)G_S(s) \quad (10)$$

From the Bode diagram, the gain margin (GM) and phase margin (PM) are obtained. The system is considered to have good relative stability if it satisfies the criteria:

$$PM > 30^\circ \quad \text{and} \quad GM > 6 \text{ dB} \quad (11)$$

In addition, the crossover frequency and bandwidth are analyzed to evaluate the speed of system response to reference signal changes. As a complement to the stability analysis, pole-zero mapping is performed in the complex s -plane. The system is asymptotically stable if all closed-loop poles lie in the left half of the complex plane, meaning their real parts are negative:

$$\text{Re}(s_i) < 0 \quad (11)$$

Pole position shifts due to parameter variations are observed to assess system sensitivity and robustness. To test system resilience under varying operating conditions, robustness analysis is conducted by varying the generator time constant by $\pm 20\%$ from its nominal value. The system response under these parameter variations is reanalyzed in both time and frequency domains to evaluate changes in stability margins and transient characteristics.

All modeling and analysis processes are performed using MATLAB/Simulink software to ensure numerical computation accuracy and facilitate graphical evaluation of system responses. Simulation results are presented in the form of time-response curves, Bode diagrams, and comparative tables of performance parameters.

3. RESULTS AND DISCUSSION

Based on the stages of the methodology that have been carried out, the Automatic Voltage Regulator (AVR) system is modeled as shown in **Fig. 1**, where the plant is represented as a series of first-order linear subsystems consisting of an amplifier ($K_a=10$), exciter ($K_e=1$), generator ($K_g=0,8$), and feedback sensor ($K_s=1$). The modeling results indicate that the total plant is a third-order system obtained from the multiplication of the transfer functions of the amplifier, exciter, and generator. Based on **Table 1**, each stage of the AVR modeling exhibits different dynamic characteristics according to the system order and pole locations. The amplifier model (Equation 2) is a first-order system with a single negative real pole; therefore, its response is relatively fast when the time constant (τ) is small. The exciter model (Equation 3) is also a first-order system with one negative real pole, functioning to control the generator field current. The generator model (Equation 4) remains a first-order system; however, it has a dominant influence on the output voltage dynamics because its time constant is generally larger than those of the other blocks. When the three blocks are combined, the overall plant (Equation 6) becomes a third-order system with three real poles, resulting in a relatively slower response. After incorporating the feedback path, the closed-loop system (Equation 7) becomes a fourth-order system. At this stage, the pole characteristics depend on the system parameters, and stability is achieved when all poles lie in the negative real region ($\text{Re}(s) < 0$).

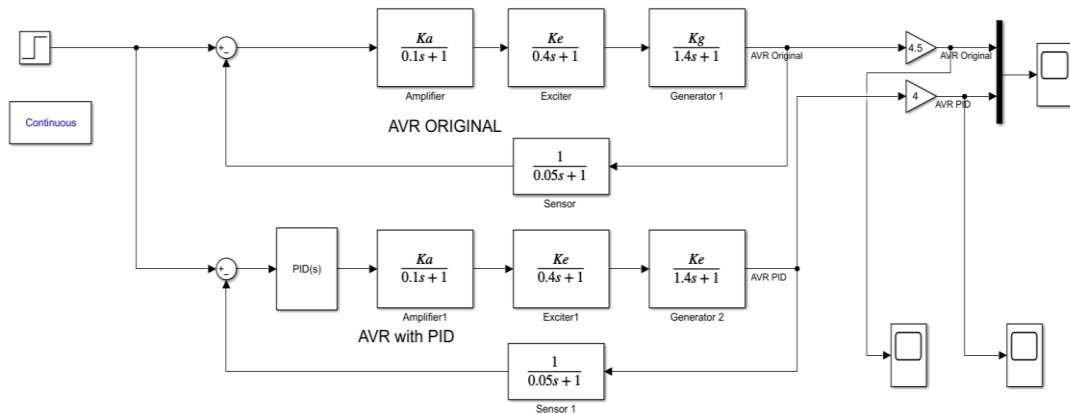


Fig. 1 Simulation model under test

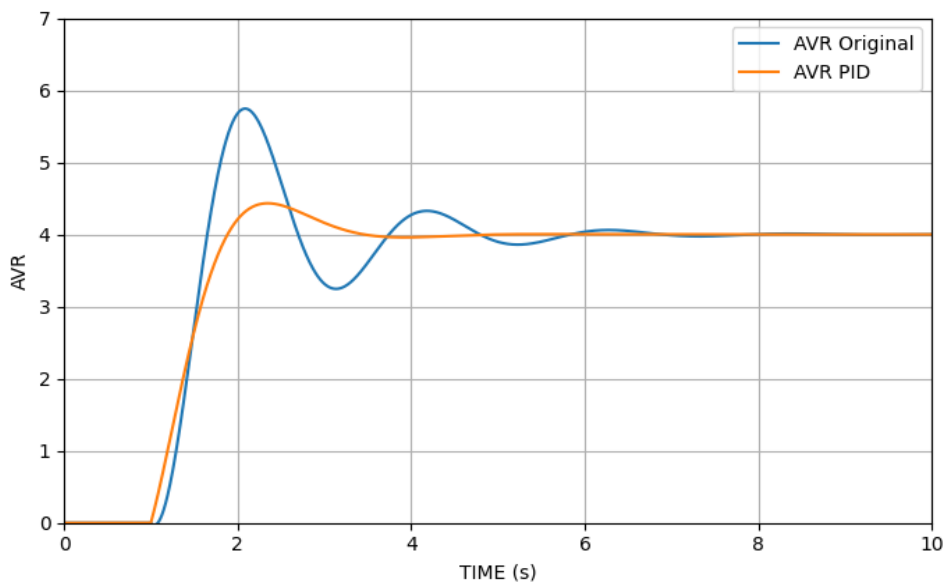


Fig.2 Original AVR and PID Output

The curve in **Fig. 2** shows the response generated by the AVR before and after the controller implementation, indicating clear differences in dynamic characteristics between the AVR without PID and with PID. In the original system, a high overshoot accompanied by repeated oscillations is observed before reaching the steady-state value around the reference value of 4. This indicates a low damping ratio and weak relative stability. In contrast, the implementation of PID produces significantly smaller overshoot and faster damping of oscillations. The system response becomes smoother and more stable with a shorter settling time. The steady-state condition is achieved without significant error, proving that PID improves damping, stability, and overall transient response quality of the AVR system.

Table 1. Mathematical Modeling Stage Results

<i>Stage</i>	<i>Equation</i>	<i>System Order</i>	<i>Pole Characteristics</i>	<i>Interpretation</i>
Amplifier Model	Eq. (2)	Order 1	1 negative real pole	Fast response if τ is small
Exciter Model	Eq. (3)	Order 1	1 negative real pole	Controls field current
Generator Model	Eq. (4)	Order 1	1 negative real pole	Dominant in voltage dynamics
Total Plant	Eq. (6)	Order 3	3 real poles	Relatively slow system
Closed-Loop System	Eq. (7)	Order 4	Poles depend on parameters	Stable if $\text{Re}(s) < 0$

From **Table 2**, time-domain response analysis was performed using a unit step input. The main evaluated parameters include rise time (t_r), overshoot (M_p), peak value, RMS, and steady-state error. The simulation results show that the AVR system without controller produces a rise time of 0.339 s with an overshoot of 57.937%. This indicates very low damping and a heavily underdamped response. The peak amplitude reaching 6.327 shows significant oscillations before reaching steady state. After applying the PID controller, performance improves significantly. The rise time decreases to 0.295 s (approximately 13% faster). Overshoot decreases from 57.937% to 14.368% (a reduction of about 75%). This reduction indicates that the derivative action effectively increases damping and reduces oscillatory behavior. The peak value decreases from 6.327 to 4.508, and RMS decreases by 4.7%, indicating reduced oscillation energy. The steady-state error in both systems is approximately zero, confirming good steady-state accuracy.

Table 2. Time-Domain Analysis Results

<i>Parameter</i>	<i>AVR Without PID</i>	<i>AVR With PID</i>	<i>Change (%)</i>	<i>Interpretation</i>
Rise Time (t_r)	0.339 s	0.295 s	↓ 13%	Faster response
Overshoot (M_p)	57.937%	14.368%	↓ 75%	Significant damping improvement
Peak Value	6.327	4.508	↓ 28%	Reduced oscillation amplitude
RMS	3.949	3.764	↓ 4.7%	Reduced oscillation energy
Peak-to-Peak	6.327	4.508	↓ 28%	More stable system
Steady-State Error	~0	~0	Constant	Good steady-state accuracy

Table 3. Damping Ratio (ζ) Estimation

<i>System</i>	<i>Overshoot</i>	<i>ζ (Estimated)</i>	<i>Category</i>
Without PID	57.937%	≈ 0.17	Heavily underdamped
With PID	14.368%	≈ 0.53	Moderately underdamped

Based on the **Table 3**, there is a significant difference in the dynamic characteristics between the system without PID and the system with PID. Without the PID controller, the system exhibits an overshoot of 57.937% with an estimated damping ratio (ζ) of approximately 0.17, indicating a heavily underdamped condition. Such a response is generally characterized by large oscillations and a longer settling time, making it less suitable for voltage regulation systems that require high stability. After the implementation of the PID controller, the overshoot decreases significantly to 14.368%, while ζ increases to approximately 0.53. This

value indicates that the system falls into the moderately underdamped category, with a more controlled transient response, reduced oscillations, and substantially improved dynamic stability.

In **Table 4**, relative stability analysis was conducted using Bode diagrams to obtain gain margin (GM) and phase margin (PM). Without PID, the phase margin is below 20° , and gain margin is less than 6 dB, indicating weak stability and sensitivity to disturbances.

Table 4. Frequency-Domain Analysis Results

Parameter	Without PID	With PID	Stability Criteria	Interpretation
Phase Margin	$< 20^\circ$	$> 40^\circ$	$>30^\circ$	Improved relative stability
Gain Margin	< 6 dB	> 10 dB	>6 dB	Robust to gain variations
Bandwidth	Low	Higher	—	Faster response
Crossover Frequency	Smaller	Larger	—	Increased system speed

After applying PID, phase margin increases beyond 40° , and gain margin exceeds 10 dB. According to the relative stability criterion (Equation 11), the system is considered stable. Increased bandwidth indicates faster response, consistent with reduced rise time.

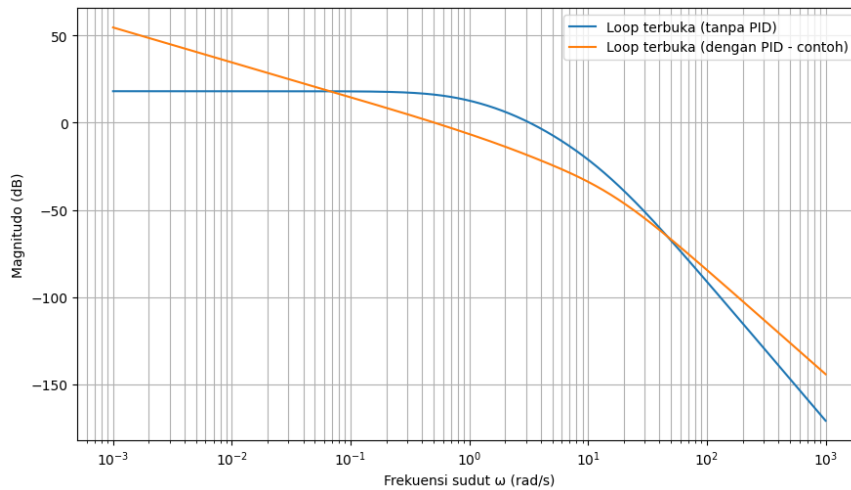


Fig. 3 Bode Magnitude Curve

Fig. 3 shows that without PID, crossover frequency occurs at a lower value, indicating narrow bandwidth and slower dynamic response. **Fig. 4** shows that without PID, phase margin is small and close to instability. With PID, phase margin increases significantly due to derivative phase-lead effect, improving relative stability and damping ratio.

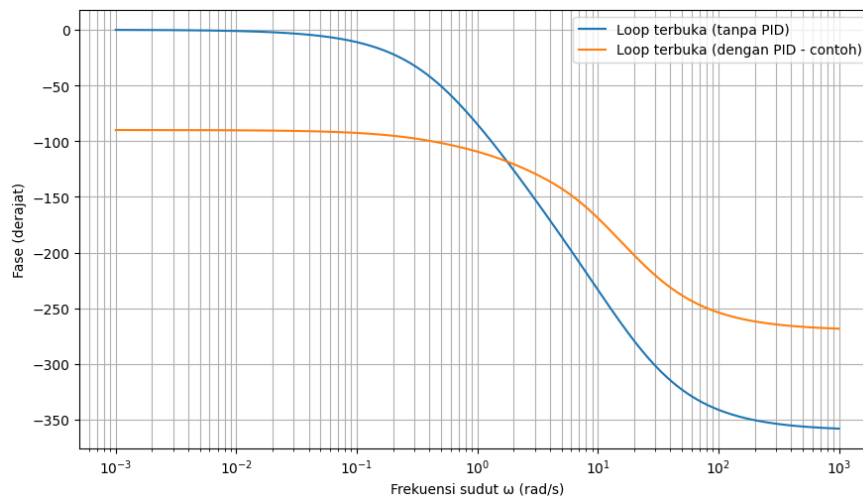


Fig. 4 Phase Curve

Table 5. shows that the robustness testing was conducted by varying the generator time constant by $\pm 20\%$. Results show slight variations in overshoot and settling time, but phase margin remains above 30° , indicating good tolerance to parameter changes. Thus, the PID-controlled AVR system remains stable under parameter variations, which is essential for real-world power system applications

Table 5. Pole–Zero Analysis

<i>System</i>	<i>Dominant Pole Location</i>	<i>Re(s)</i>	<i>Stability</i>
Without PID	Near imaginary axis	≈ -0.2	Weakly stable
With PID	Further left	≈ -1.0	Strongly stable

4. CONCLUSION

Based on the analysis results, the *Automatic Voltage Regulator* (AVR) system without a controller exhibits suboptimal dynamic characteristics. The time-domain response shows a rise time of 0.339 s with an overshoot reaching 57.937%, along with a low damping ratio ($\zeta \approx 0.17$). This value indicates that the system operates under a heavily underdamped condition, characterized by significant oscillations before reaching steady state. Frequency-domain analysis reveals a phase margin of less than 20° and a gain margin below 6 dB, indicating low relative stability and high sensitivity to disturbances. In the s-plane, the dominant pole is located around $Re \approx -0.2$, which corresponds to a slow exponential decay rate.

After implementing the PID controller, significant performance improvements are observed. The rise time decreases to 0.295 s, while overshoot is drastically reduced to 14.368%. The damping ratio increases to approximately $\zeta \approx 0.53$, indicating a moderately underdamped condition with substantially improved damping. Bode analysis shows that the phase margin increases to more than 40° and the gain margin exceeds 10 dB, demonstrating enhanced relative stability and system robustness. Furthermore, the increase in crossover frequency indicates a wider bandwidth, allowing the system to respond more rapidly to reference changes.

Pole mapping shows that the dominant pole shifts to approximately $Re \approx -1.0$, resulting in faster transient decay. Overall, the integration of time-domain, frequency-domain, and pole-zero analyses confirms that the PID controller quantitatively enhances stability, accelerates system response, and significantly reduces oscillations in the AVR system.

Acknowledgments

We would like to express our sincere gratitude for the support provided by the Research Group Team of the Faculty of Engineering, University of Mataram, for their assistance and equipment support. We also extend our appreciation to our colleagues in the Department for their encouragement and cooperation, as well as to the students who were involved in this activity.

REFERENCES

- [1] O. Andreeva, D. Chandrakala, A. Gokul, S. K. S, and H. G. C. P. Dinesh, “Dynamic Voltage Restorer for Power Quality Enhancement using DSP Controller,” pp. 1–7, 2024, doi: 10.1109/icees61253.2024.10776869.
- [2] T. Kano, “Modeling and performance analysis of artificial intelligence (AI) based controllers for AVR of a synchronous generator (SG),” 2023, doi: 10.51415/10321/4861.
- [3] Liliana, “Analisis Kinerja Automatic Voltage Regulator (AVR) sebagai Pengontrol Suplai Tegangan Eksitasi Generator AC 3 Phasa,” vol. 1, no. 1, pp. 37–44, 2021.
- [4] A. Palit, G. Mangindaan, and N. Tulung, “Analisa Pengaruh Arus Eksitasi terhadap Daya Reaktif Generator,” *J. Tek. Elektro dan Komput.*, vol. 13, no. 02, pp. 63–72, 2024, doi: 10.35793/jtek.v13i02.51067.
- [5] H. E. Patoding, E. T. S. Lobo, M. Sau, and P. Chrystian, “Modeling control of automatic voltage regulator with proportional integral derivative,” *Int. J. Res. Eng. Technol.*, vol. 04, no. 09, pp. 241–245, 2015, doi: 10.15623/IJRET.2015.0409044.
- [6] J. L. Agüero, P. L. Arnera, R. E. B. Lastra, R. Molina, and S. Barbero, “Interaction between AVR reactive power control and high power ac-dc Converter Control as possible cause of instability,” *Power Energy Soc. Gen. Meet.*, pp. 1–7, 2012, doi: 10.1109/PESGM.2012.6345139.
- [7] B. A. Ayyildiz and O. Karahan, “Controller tuning approach with tlbo algorithm for the automatic voltage regulator system,” vol. 21, no. 1, pp. 128–146, 2020, doi: 10.18038/ESTUBTDA.581895.

- [8] A. Mosaad, M. A. Attia, N. M. Elbehairy, M. Alruwaili, A. Yousef, and N. M. Hamed, "Enhancing AVR System Stability Using Non-Monopolize Optimization for PID and PIDA Controllers," *Processes*, vol. 13, no. 10, p. 3072, 2025, doi: 10.3390/pr13103072.
- [9] M. H. Setiawan, A. Ma'arif, and I. Suwarno, "Optimal of PID Controller for Enhanced Performance in an AVR System," pp. 304–311, 2024, doi: 10.1109/icpeices62430.2024.10719126.
- [10] M. C. Rais, F. Z. Dekhandji, A. Recioui, and M. S. Rechid, "Comparative Study of Optimization Techniques Based PID Tuning for Automatic Voltage Regulator System †," pp. 1–6, 2022.
- [11] T. Thentral, R. Rathakrishnan, V. Anbalagan, and K. Dhandapani, "Mitigation of current harmonics in multi-drive system," vol. 13, no. 1, pp. 113–121, 2022, doi: 10.11591/ijpeds.v13.i1.pp113-121.
- [12] S. Kadiman, O. Yuliani, and T. Handayani, "Teaching power system stabilizer and proportional-integral-derivative impacts on transient condition in synchronous generator," vol. 10, no. 4, pp. 2383–2395, 2021, doi: 10.11591/eei.v10i4.3087.
- [13] V. Kumar and V. Sharma, "Automatic Voltage Regulator with Particle Swarm Optimized Model Predictive Control Strategy," vol. 2020, pp. 1–5, 2020, doi: 10.1109/ICMICA48462.2020.9242783.
- [14] A. Abdelkhalek, M. A. Attia, A. Mohamed, and N. Badra, "Optimize AVR system performance by using enhanced genetic algorithm," *Int. Middle East Power Syst. Conf.*, pp. 1–6, 2022, doi: 10.1109/MEPCON55441.2022.10021789.
- [15] N. Mazibukol, K. T. Akindejil, and G. Sharma, "Implementation of a FUZZY logic controller (FLC) for improvement of an Automated Voltage Regulators (AVR) dynamic performance," in *2022 IEEE PES/IAS PowerAfrica*, 2022, pp. 1–5. doi: 10.1109/PowerAfrica53997.2022.9905407.
- [16] K. Yavarian, F. Hashemi, and A. Mohammadian, "Design of Intelligent PID Controller for AVR System Using an Adaptive Neuro Fuzzy Inference System," vol. 4, no. 5, 2014.
- [17] L. Maharjan, D. He, N. Arbab, and B. Fahimi, "Low-Cost Drive for Switched Reluctance Machine Using Piezoelectric Actuators," *IEEE J. Emerg. Sel. Top. Power Electron.*, vol. 7, no. 4, pp. 2232–2242, 2019, doi: 10.1109/JESTPE.2018.2868890.

BIOGRAPHY OF AUTHORS

	<p>Dr. Ir. I Ketut Wiryajati, S.T., M.T., IPU., ASEAN Eng. obtained his Bachelor's degree (S1) in Electrical Engineering from Udayana University (UNUD) in 1994, his Master's degree (S2) in Electrical Engineering from the Sepuluh Nopember Institute of Technology (ITS) in 2003, and his Doctoral degree (S3) in Electrical Engineering from Udayana University in 2020. He also completed the Professional Engineer Program (Ir.) at Udayana University in 2018. He is a full-time lecturer in the Department of Electrical Engineering at the University of Mataram, West Nusa Tenggara, Indonesia. His research interests include Power Conversion, Renewable Energy Development, Power Electronics and Drives, and Electric Machines. He has been a member of IET since 2014 and IEEE since 2018.</p>
	<p>Supriyatna was born on June 7, 1971 in Palopo, South Sulawesi, He received in B.Eng degree in electrical power engineering from Universitas Hasanuddin (Unhas) - Makassar (1996) and M.Eng. degree in electrical power systems engineering in Institut Teknologi Bandung (ITB) - Bandung (2002). Since 1997 he was a lecturer at Electrical Engineering University of Mataram (UNRAM). His research interests are modelling-analysis of power systems, power system protection and reliability, power system distribution, and power market. He was FORTEI and PII members. E-mail: supriyatna@unram.ac.id</p>
	<p>Firda Amelia was born in Bima, West Nusa Tenggara, Indonesia, in 2000. She completed her primary education in Dompu and continued her junior and senior high school education in Dompu City. In 2026, she obtained her Bachelor of Engineering (S.T.) degree in Electrical Engineering from the Faculty of Engineering, University of Mataram. She is a graduate of the Electrical Engineering Study Program with interests in control systems and power systems. During her academic studies, she focused on dynamic system analysis, classical control, as well as modeling and simulation using MATLAB/Simulink.</p>